

June 2011

Design and application of a test setup for measuring phosphor annealing processes

Robert Koch

Division of Combustion Physics
Lund University



Fachhochschule Jena
University of Applied Sciences Jena

Bachelor of Science Thesis

Fachhochschule Jena

Fachbereich SciTec

DESIGN AND APPLICATION OF A TEST SETUP
FOR MEASURING PHOSPHOR ANNEALING
PROCESSES

Bachelorarbeit

vorgelegt von:	Robert Koch
geboren am:	23.03.1985 in Meiningen
Studiengang:	Physikalische Technik
Matrikelnummer:	540514
Hochschulbetreuer:	Prof. Dr. rer. nat. B. Ploss
Betreuer in Lund:	Dipl.-Phys. C. Knappe
Abgabedatum:	27.06.2011

© 2011

Dieses Werk einschließlich seiner Teile ist **urheberrechtlich geschützt**. Jede Verwertung außerhalb der engen Grenzen des Urheberrechtsgesetzes ist ohne Zustimmung des Autors unzulässig und strafbar. Das gilt insbesondere für Vervielfältigungen, Übersetzungen, Mikroverfilmungen sowie die Einspeicherung und Verarbeitung in elektronischen Systemen.

© Robert Koch

Lund Reports on Combustion Physics, LRCP-147

ISRN LUTFD2/TFC-147-SE

ISSN 1102-8718

Lund, Sweden, June 2011

Robert Koch

Division of Combustion Physics

Department of Physics

Faculty of Engineering LTH

Lund University

P.O.Box 118

S-221 00 Lund, Sweden

Populärvetenskaplig Sammanfattning

Detta arbete handlar om att utveckla och förbättra en försöksuppställning som kan mäta laser-inducerad fosforescens både spektralt och tidsupplöst. Ämnet som emitterar fosforescensen befinner sig i en kalibreringsugn som kan värmas till olika temperaturer vilket möjliggör studier av irreversibla åldringsprocesser i ämnet som funktion av temperatur och tid. Fosforescens är den långa efterglöd som fosforescerande material ger ifrån sig efter att elektroner i materialet exciterats till högre elektroniska nivåer. Den har relativt lång varaktighet till följd av delvis förbjudna övergångar från triplet till singlet-övergångar, till skillnad från den snabbare fluorescensen som härstammar från singlet till singlet-övergångar. Med hjälp av termografiska fosforer bestäms t.ex. temperaturen beröringsfritt på svåråtkomliga ytor i förbränningsmiljö.

I det här arbetet ligger fokus på en sådan termografisk fosfor, nämligen $\text{La}_2\text{O}_2\text{S:Eu}$ - som lämpar sig bra för temperaturmätning i motormiljö upp till $300\text{ }^\circ\text{C}$. Undersökningar genomfördes för olika dopningskoncentrationer av Eu (2at% och 8at%) som påverkar det känsliga temperaturområdet hos fosfor. Det antas att de mest intressanta effekterna i fosfor inträffar strax efter att fosfor har exponerats för höga temperaturer. I ett tidigt skede av experimenten identifierades den långa uppvärmningstiden av fosfor i ugnen som en av huvudfelkällorna. En viktig deluppgift av arbetet blev därför att designa en förbättrad provhållare till ugnen som minimerar denna tid så att relevanta mätningarna kan påbörjas tidigare. Mot slutet av detta bachelorprojekt utfördes de första testmätningar med den nya försöksuppställningen och resultaten utlovar intressanta möjligheter att studera fosfors åldringsbeteende framöver.

Acknowledgment

I would like to thank my supervisor in Jena Prof. Bernd Ploss for the support in preparation of my stay in Lund as well as for the support during the thesis.

I would like to thank Prof. Marcus Aldén for giving me the possibility to write my bachelor thesis at the Combustion Physics Division.

I would like to thank particularly Christoph Knappe for his invitation to Lund and for his faithful, competent and patient supervision. I had a great, inspiring and productive time in the 'phosphor group', managed by him. Also, I would like to thank him for the support for writing the thesis.

I would like to thank Fahed Abou Nada for his continuous support and his help for writing Matlab codes and for solving problems.

I would like to thank all members of the Combustion Physics Division for the pleasant working atmosphere.

Last, I would like to thank my parents for supporting my stay in Lund.

Contents

1	Introduction	7
2	Physical Principles of Luminescence	8
3	Experimental Setup	12
4	Results and Discussion	15
4.1	Sample Holder Design and Warm-Up-Time Reduction	15
4.2	Time-Gated Spectral Investigation using the CCD camera behind the Spectrometer	21
4.2.1	Spectra Processing	21
4.2.2	Trigger Delay for the CCD Camera	25
4.3	Time Decay Investigations at 538 nm Phosphor Emission	28
4.3.1	Influence of the Phosphor Preparation Time on the Intensity	28
4.3.2	Investigation of the Intensity Ratio between Peak and Phosphorescence from the PMT Decay Curves	29
5	Summary and Outlook	30

1 Introduction

A phosphor is a solid luminescent material or a powder synthesized for purpose of practical application [5]. Phosphorescence is defined as an extended afterglow following excitation, that originates from a quantum mechanically forbidden triplet-to-singlet transition [5].

Laser Induced Phosphorescence (LIP) is a remote measurement method for surface temperatures. LIP is used for example for thermometry in engines or gas turbines in order to study heat transfer processes to the surface walls, which in the long run can lead to improved efficiency.

A phosphorescent material (phosphor) can be excited by laser radiation at a certain wavelength and emits spectra at higher wavelengths. The spectral intensity distribution as well as time decay of the phosphorescence is dependent on the temperature.

LIP is a common probing tool in demanding environments such as combustion research. It has several advantages compared to other temperature measurement techniques:

- it has a high temporal resolution
- it is a non-contact method and
- it has a higher accuracy than other remote standard techniques, such as pyrometry [2].

There is a rich variety of thermographic phosphors suitable for LIP. Altogether they cover a range that stretches from cryogenic temperatures up to 1700 °C [4][1]. Concerning thermometry in engines, the $\text{La}_2\text{O}_2\text{S}:\text{Eu}$ -phosphor is especially applicable, because its decay time changes several orders of magnitude between room temperature and 300 °C. This guarantees a very high temperature precision. The temporal resolution, which is in the same order of magnitude as the phosphorescence decay time, ranges from nanoseconds to microseconds and can thus be employed for surface temperature investigation in combustion in engines, where changes typically occur within several tens to hundreds of microseconds.

In previous experiments the following phenomenon was observed: the fresh phosphor coating delivered a higher decay intensity at certain wavelengths than after one hour of engine operation. Later on the excited decay signal decreased even further to almost zero intensity after two days rest.

In order to apply the $\text{La}_2\text{O}_2\text{S}:\text{Eu}$ -phosphor in environments with varying temperatures it is most important to investigate

- if the phenomenon is degeneration of the phosphor
- if the phenomenon is reproducible and
- if it could be made predictable for certain temperatures.

The goal of this thesis is to enable the mentioned investigations. This goal is put into practice by developing, optimizing and testing an experimental setup.

2 Physical Principles of Luminescence

In the following section will be answered mainly two questions:

- What can happen to excited luminescent molecules?
- How can phosphorescence work for temperature measurement?

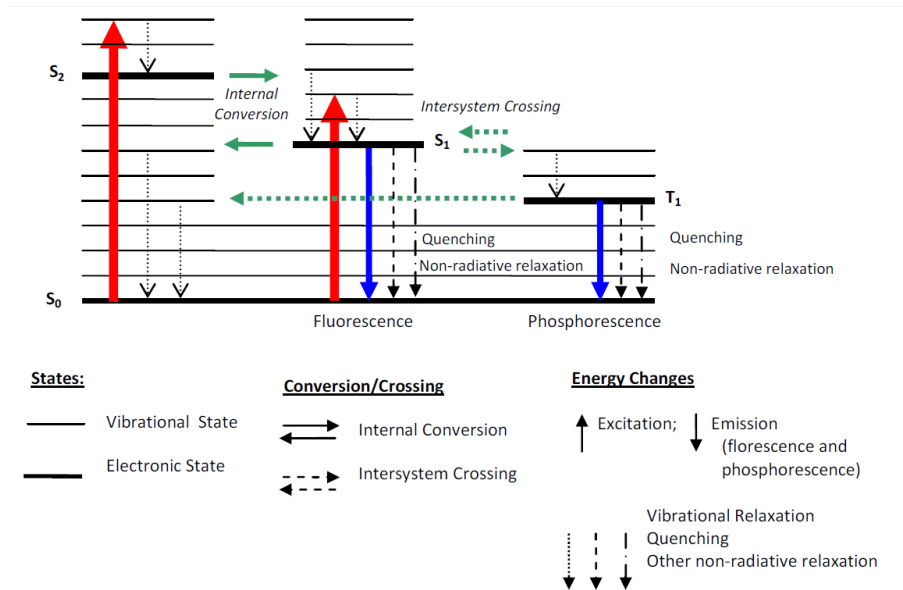


Figure 1: Jablonski energy level diagram [3]: The red arrows represent excitation to vibrational states by photons, the longer blue arrow is fluorescence, the shorter blue arrow is phosphorescence. Although both blue arrows stand for emission of a photon, the light frequency is higher for the fluorescence.

In the Jablonski energy level diagram (figure 1) is shown, how an atom is excited and how it emits its energy. An incident photon causes the electron to jump to an excited state, represented by the red arrow. There are several forms of energy emission:

- emission of photons with the energy $h \cdot \nu = \Delta E$ (difference in the energy level); these emissions are represented by the blue arrows,
- energy transfer via crystal lattice phonons
- other energy transfer mechanisms like quenching, internal conversion, inter system crossing

Phosphorescence is caused by electronic transitions between a very long lived state and a lower energy level during de-excitation, while fluorescence is a radiative transition of an orbital electron between a short lived state and the ground state. That is why fluorescence has a shorter lifetime than phosphorescence. Also, excited atoms can interact with each other and with the surroundings, which has influence on the type of emission. If the influence is thermally driven, it makes the emission of the phosphorescent material sensitive to temperature.

Most thermographic phosphors show an exponential signal decay that can be estimated by

$$I = I_0 \exp\left(\frac{-t}{\tau}\right) + C,$$

where I_0 , τ and C are constants. I_0 is the initial intensity of phosphorescence. In practice I_0 is interfered by the laser peak. It can be calculated by fitting the mentioned exponential function to the decay signal. τ is the lifetime of the phosphor. The lifetime describes how long it takes the phosphorescence signal to decay to $1/e$. The offset C has to be subtracted before fitting, calculation of I_0 and τ . To start measurement of the Photo Multiplier Tube signal view microseconds before laser excitation is very important for calculating C .

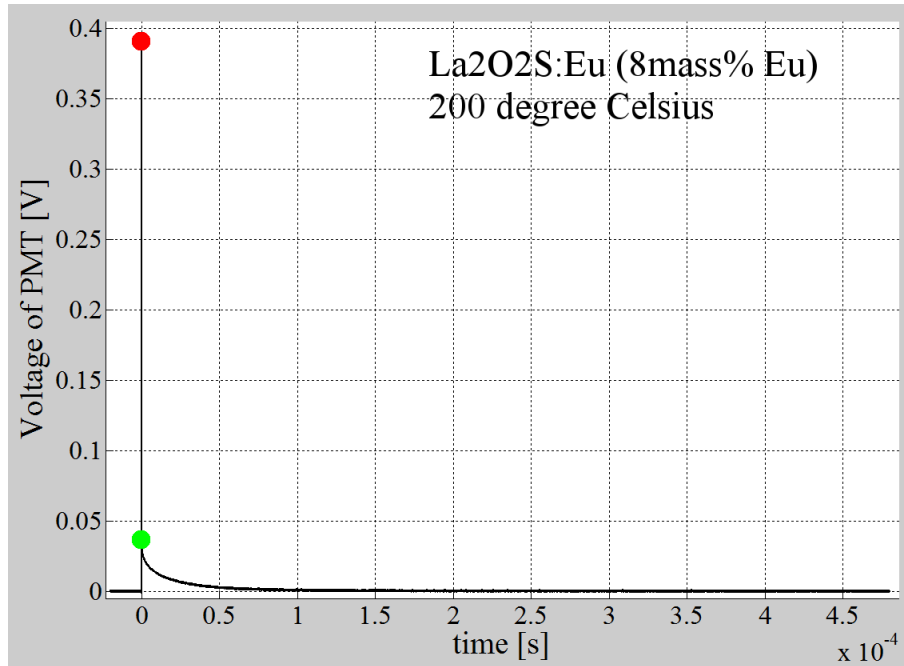


Figure 2: Example for a decay curve, that consists in general of two parts: a peak caused by fluorescence and laser spurious light and second the exponential decay, caused by the phosphorescence. The red dot marks the maximum intensity, the green dot represents I_0 . The ratio is calculated by dividing the voltage of the green dot by the voltage of the red dot.

The peak is much too strong and makes the signal decay evaluation more noisy, because the detector has a limited dynamic range and if the detector should not be saturated with the peak, the rest of the signal becomes very weak. The signal, that is detected, consists of the decay of phosphorescence and part of the laser intensity, that is reflected by the phosphor and also some fluorescent emission.

The following figure shows the application of thermographic phosphors for temperature measurement. A calibration at well-known temperatures is necessary to match unknown temperatures by decay lifetimes.

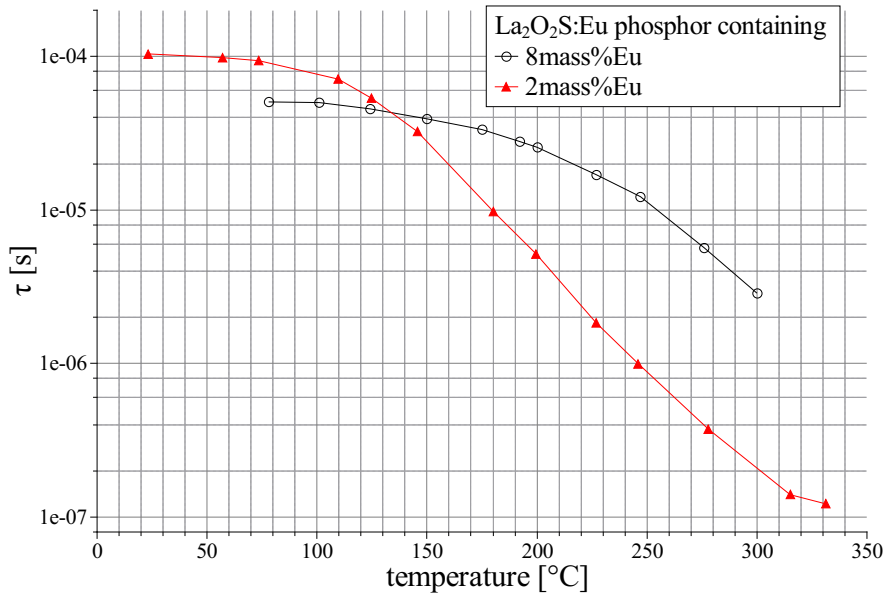


Figure 3: Temperature calibration curves: phosphor lifetimes τ over temperature, emission at 540 nm for two different europium concentrations.

In figure 3 is shown, that within the given temperature range the phosphor lifetimes τ changes by three orders of magnitude for 2mass% Eu phosphor and about only one order of magnitude for 8mass% Eu phosphor. The calibration of 8mass% Eu phosphor could be extended for higher temperatures to increase its orders of magnitude. The 8mass% Eu phosphor probably has a measurement range, that is shifted to higher temperatures.

3 Experimental Setup

This section is dedicated to provide informations on the experimental details:

The experimental setup used during this work is introduced and explained.

The setup was composed to investigate in the phosphorescence of $\text{La}_2\text{O}_2\text{S}:\text{Eu}$ in two ways:

- on one hand by recording a signal around 538 nm with high temporal resolution by using the PMT and the oscilloscope and
- on the other hand by recording spectra in a certain wavelength range with the spectrometer

The fundamental wavelength of the Nd:YAG laser is 1064 nm. The Quantel Brilliant B laser has a pulse frequency of 10 Hz, a pulse FWHM duration of ≈ 7 ns and its pulse energy was set to 3 mJ. The fundamental frequency is doubled in a 2ω unit and that means, the wavelength is divided by two to 532 nm (2nd harmonic). In the 3ω unit the 2nd harmonic is mixed with the fundamental wavelength to get 355 nm. A prism separates the 532 nm light from the 355 nm light and also reflects the beam into the direction of the furnace. The beam hits the phosphor sample inside the furnace, that can be set to various temperatures. Set points can be adjusted at a temperature controller. For measurement of the temperature inside the chamber a K-type thermocouple is used.

Diffuse phosphorescent light is emitted by the sample and is collected by two lenses (focal lengths $f_1 = 152$ mm and $f_2 = 200$ mm, diameters $d_1 = d_2 = 50$ mm). The collecting lenses guide the light to the PMT as well as to the spectrometer.

The phosphorescence emits into the whole room angle. The light has to be collected by lenses to increase the signal to noise ratio at both, PMT and spectrometer, because the detector surfaces cover only a small fraction of the whole room angle. Also, the spectrometer can detect incident light only within a certain acceptance angle. The focal length of the lens is chosen to illuminate the whole detector surface. For example, the PMT surface has approximately the diameter of the laser spot. It is reasonable to image the laser 1:1 by choosing an according focal length.

The 532 nm light has to be separated and absorbed by a beam dump, because it is very close in wavelength to the 538 nm phosphorescence emission, that is collected using the Photo Multiplier Tube (PMT) behind a 540 nm bandpass filter (FWHM = 10 nm). If the 532 nm was not blocked, there was a lot too much laser light at the PMT, because the laser provides a lot more energy per time unit than the phosphorescence. In front of the PMT as well is a high pass filter (blocking low wavelengths), that has its edge (50% transmission) at 400 nm to reduce the intensity of the 355 nm laser wavelength drastically.

In front of the Spectrometer is a 45° laser mirror, that reflects about 99% of 355 nm light at 45° . Its angle can be slightly varied to increase laser intensity in the spectrum, because

reflectivity decreases for mirror angles that vary from 45° .

By turning the spectrometers grating there are different spectral ranges available. The grating has $300 \text{ lines} \cdot \text{mm}^{-1}$ and that means it can see a wider range with less spectral power of resolution than the $1200 \text{ lines} \cdot \text{mm}^{-1}$ grating. Using the $300 \text{ lines} \cdot \text{mm}^{-1}$ grating two different but overlapping ranges were chosen ($352 \text{ nm} \dots 607 \text{ nm}$; $462 \text{ nm} \dots 715 \text{ nm}$). Both ranges are necessary to cover the 3ω laser wavelength (355 nm) as well as the phosphorescence at 710 nm .

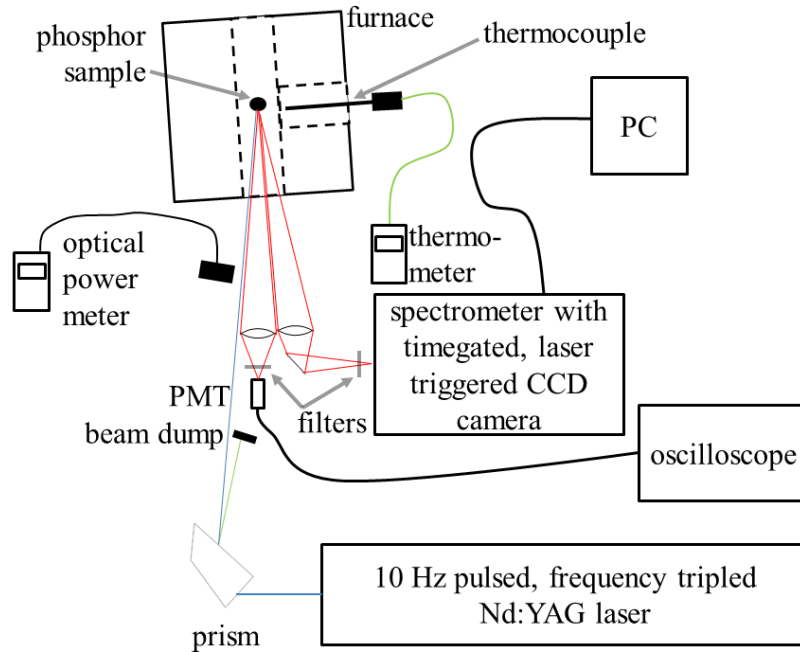


Figure 4: Sketch of the experimental setup: A Nd:YAG laser provides the energy to excite the phosphor sample in the furnace. The phosphorescent light, emitted by the sample, is collected at the PMT as well as at the spectrometer.

The spectrum is read to a 575×384 pixel CCD chip. The CCD camera time gate is adjustable and the spectrum can be investigated at different times. It is necessary to use different time windows to identify the composition of the PMT signal at 540 nm . The camera behind the spectrometer triggered by the Q-Switch of the laser. It takes at each record period 100 images with an exposure time of $500 \mu\text{s}$. The images are averaged and there is received one mean image from 100 single images. Each column of a CCD image is summed up to one intensity value, because the incident light is at each wavelength distributed along a column. Summing up the column collects the intensity information and increases the signal to noise ratio.

The PMT has a spectral response of 185 nm to 850 nm . Its rise time is 0.78 ns , which is

suitable for measuring signal changes at the nanoseconds to microseconds scale.

The PMT detects the green phosphorescent light at 538 nm and wavelengths close to this, because there are two band pass filters installed in front of it. Both of them are centered at a wavelength of 540 nm and have a FWHM of 10 nm. Additionally, a 400 nm edge filter in front of the PMT to blocks the 355 nm laser wavelength. The PMT's electrical gain was kept constant at a value of 5.3.

The PMT is connected to an oscilloscope (sampling rate $500 \frac{Ms}{s}$, input resistance 50Ω), that is triggered by the time decay signal. The point separation must not be longer than 2 ns (this is given by $500 \frac{Ms}{s}$) to resolve the laser/ fluorescence peak. For longer decays at lower temperatures, the sampling rate was reduced to $50 \frac{Ms}{s}$. A power meter is used to measure the mean laser power, which is held constant by adjusting the flash lamp- Q-switch delay.

The phosphor age time is measured with a stop watch. It is started directly after putting the sample into the furnace.

4 Results and Discussion

In the following section will be explained, why the measurements within the first thirty minutes could not be considered reliable for annealing investigation and what was done to decrease that time.

4.1 Sample Holder Design and Warm-Up-Time Reduction

The following figure shows that part, which is put into the furnace. For heat resistance it is built of steel, but it also has to meet geometrical demands.

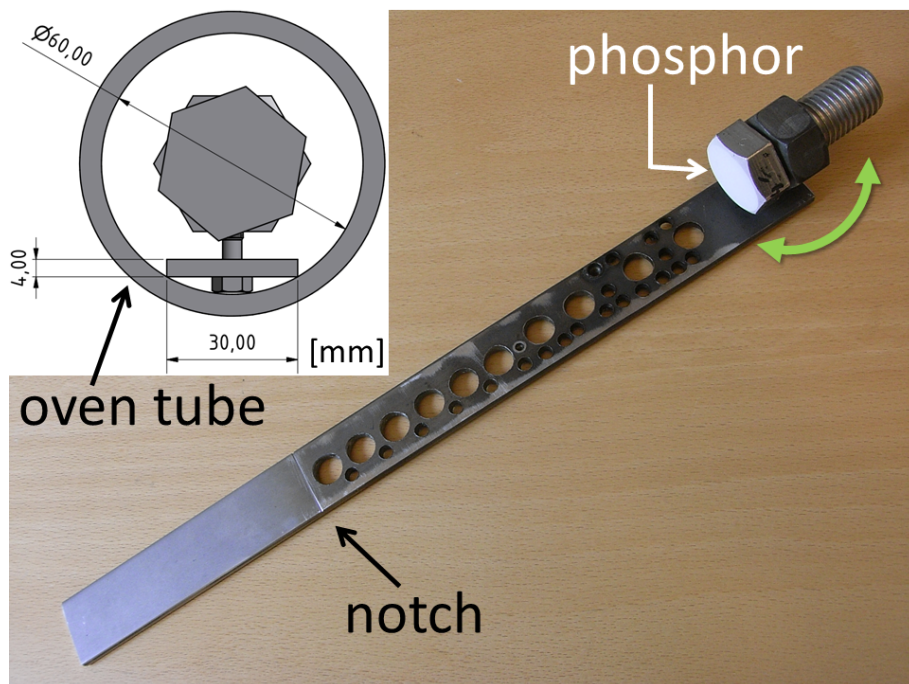


Figure 5: Image of the first phosphor sample holder prototype and a sketch of its front view in the furnace tube. The light green arrow illustrates, that the sample mount is turnable.

In figure 5 is shown the first version of a sample holder. The phosphor is coated on the top face of the head of a screw. The screw is exchangeable. A new screw is used for each phosphor coating. The holder centers the screw in the oven tube. The centering is important, because the laser beam also hits the center of the furnace tube. To make sure that the phosphor face is always at the same position, a notch is filed into the metal bar. The notch marks the entrance edge of the furnace. There are holes already drilled in the metal bar to accelerate the warming up process.

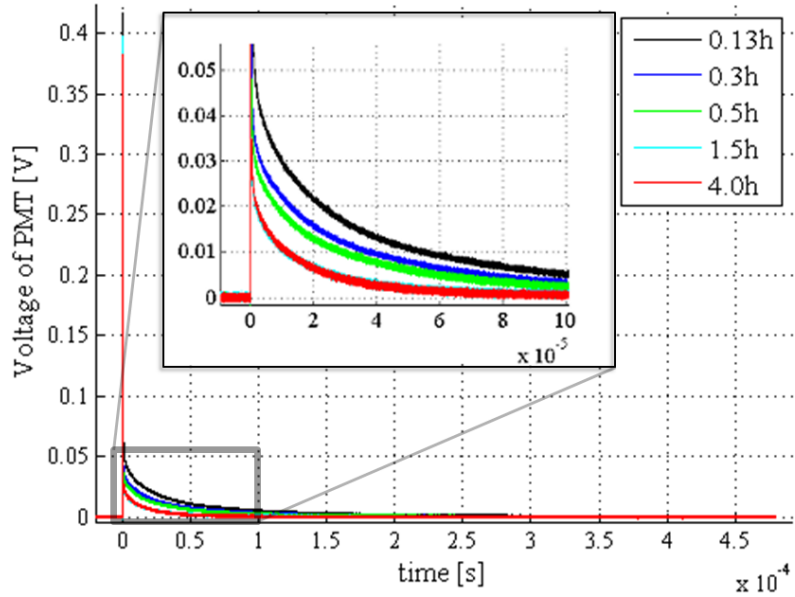


Figure 6: Phosphorescence decay at 538 nm and 200°C, emitted by $\text{La}_2\text{O}_2\text{S}:\text{Eu}$ phosphor (8mass% Eu), phosphor age as parameter.

In figure 6 there are considerable changes during the first 0.5 h and almost no changes for phosphors aged > 1.5 h. The reason for this behavior could be either a degeneration of the phosphor or a warming up process. This question leads to the investigation of the warming up time for the phosphor sample.

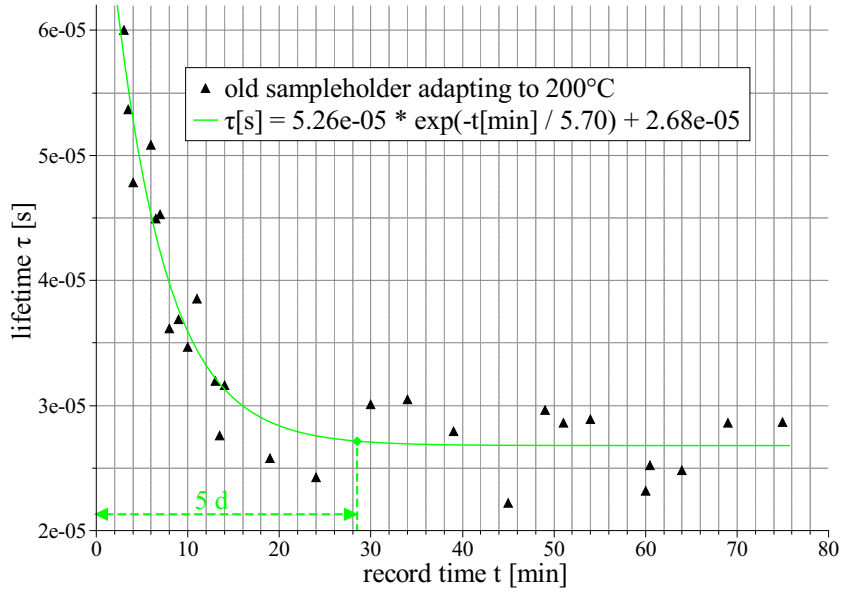


Figure 7: Warming up behavior of the 'old' sample holder, when adapting to 200 °C, 8mass% Eu. After 5*d* the deviation from the infinite stable τ is less than 1%.

In figure 7 it has been checked, how long it takes for the phosphor sample to reach furnace temperature of 200 °C. The warming up time is measured by using the phosphor itself. The oscilloscope tracks decay curves and later the lifetime τ is evaluated. When τ stabilizes, the phosphor sample has reached furnace temperature. The warming up process can be approximated by a first order exponential decay. The exponential folding time d is multiplied by factor five to get less than 1% deviation:

$$\tau = \tau_0 \exp\left(\frac{-t}{d}\right) \quad , t = 5d$$

$$\implies \frac{\tau}{\tau_0} = e^{-5} < 1\%$$

A phosphor sample is considered to be adapted to the furnace temperature, when 5*d* has passed. 5*d* in figure 7 was about 30 min. Intensity measurements and lifetime measurements can be started after this 30 min. Every annealing process faster than that cannot be detected for sure, because it interferes with the warm up.

In order to decrease the warming up time, there were taken several measures:

- drilling a lot of holes into the metal bar in order to reduce the amount of metal to be warmed up,

- cutting off the metal bar to a shorter length, that still allows to handle the sample at 300 °C without big insulation gloves,
- minimizing the contact surface between phosphor coated metal and other parts of the holder; the nut in front of the phosphor coated sheet is not tightened to reduce heat conduction,
- reducing the volume of metal, that is coated to a minimum and
- fast preheating by a hot air gun.

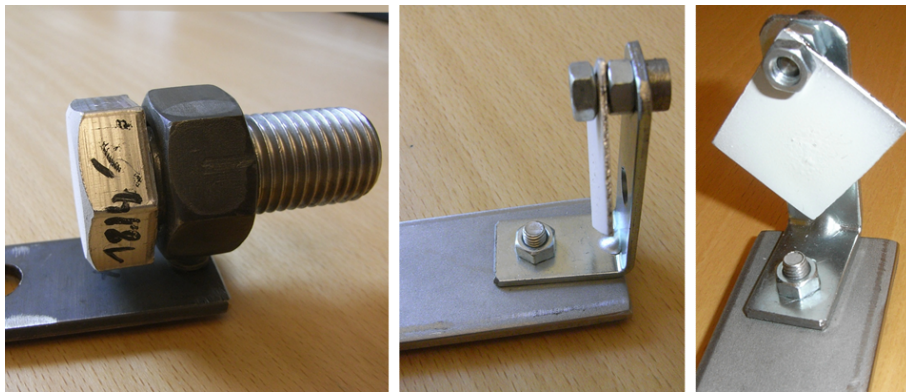


Figure 8: Left subfigure: detail of the 'old' sample holder; middle subfigure: detail of the 'new' sample holder; right subfigure: new sample holder in front view.

Finally, it was built a new sample holder (see figure 8 middle and right sub figure). It consists of a $30 \times 30 \times 1 \text{ mm}^3$ stainless steel sheet, that is coated with the phosphor and connected to a metal angle and a stainless steel bar by screws. The new construction has mainly one advantage: it is warming up more quickly to the furnace temperature.

In figure 9 two adaption curves to 200 °C are recorded.

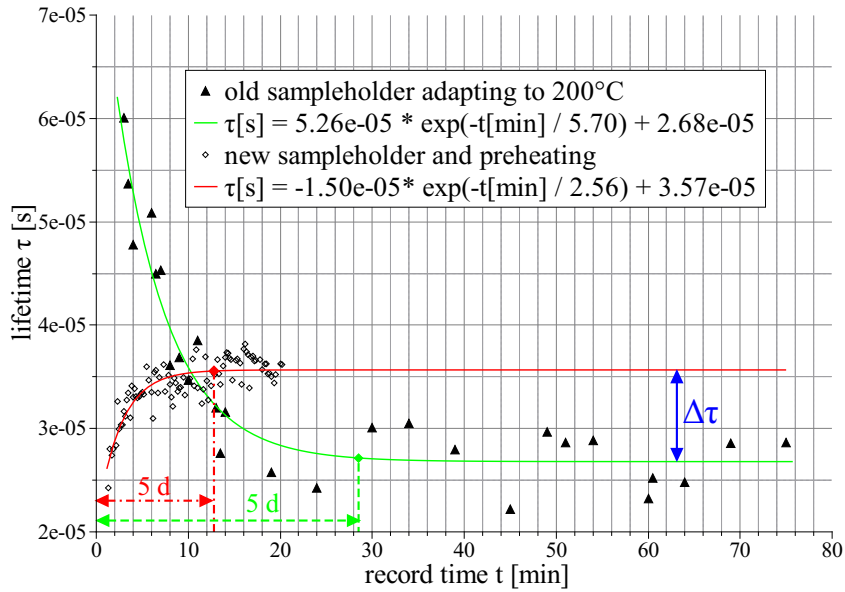


Figure 9: Comparison of warming up behaviors of 'new' and 'old' sample holder. Additionally, the 'new' holder was preheated with a hot air gun. Different Eu concentrations cause a $\Delta\tau$ (blue arrow).

The new and preheated sample holder in figure 9 takes less than half of the time of the old sample holder: about 13 min compared to about 30 min for the first prototype. There were used two different Europium concentrations: 2 mass% Eu at the new sample holder and 8 mass% Eu at the old one. According to figure 3 at 200 °C the lifetime τ should be shorter for 2 mass% Eu than for 8 mass% Eu. That explains the difference in the stabilized lifetimes $\Delta\tau$ (blue arrow in figure 9).

Actually the preheating causes a cooling down of the phosphor sample instead of the warming up, because the temperature that is reached by the hot air gun is higher than the furnace temperature.

The hot air gun is held in approximately 10 cm distance to the phosphor. It should be applied at its pitch '1' for about 2 min, when preparing for 200 °C and for less time when adapting to lower temperatures. Six different measurements for three different sample holder solutions are shown in figure 10.

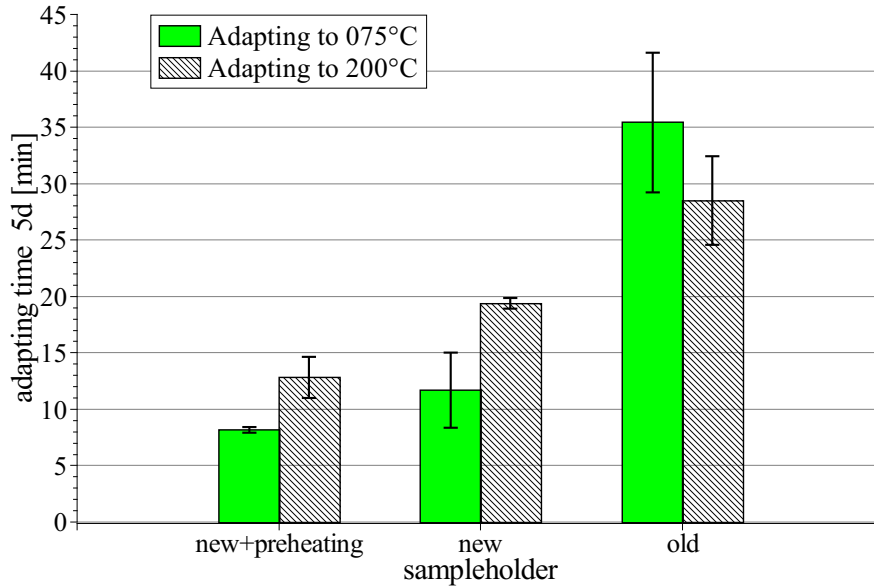


Figure 10: Summary plot of the warming up measurements: the adaptation times of different solutions for the sample holder are compared at two different temperatures.

The bar chart shows, that the adapting time for the phosphor at the old sample holder could be decreased considerably by the new one. Combined with preheating the process becomes even faster. It can be concluded, that one is on the safe side, when applying preheating with the new holder and keeping the phosphor for 15 min in the furnace before starting intensity measurements. The preheating improves the new sample holder by 30% (75 °C) and by 34% (200 °C). The adapting times 'old' to 'new + preheating' were reduced by 55% (200 °C) and 77% (75 °C).

Contrary to expectations the $5d$ for the old holder at 75 °C is greater than at 200 °C. Also the error bar is very big. It was difficult to fit an exponential decay to the dataset (old, 75 °C), because points were scattered and the trend was not very obvious. Also, the evaluation of the lifetimes was not possible or reasonable for all data points in this set.

4.2 Time-Gated Spectral Investigation using the CCD camera behind the Spectrometer

4.2.1 Spectra Processing

This section will show, how the CCD camera image can be processed to a spectrum, how the spectra look like and the spectral development in time will be compared to time decay of PMT signals.

The following figure 11 has been extracted from an article, building the base for wavelength calibration.

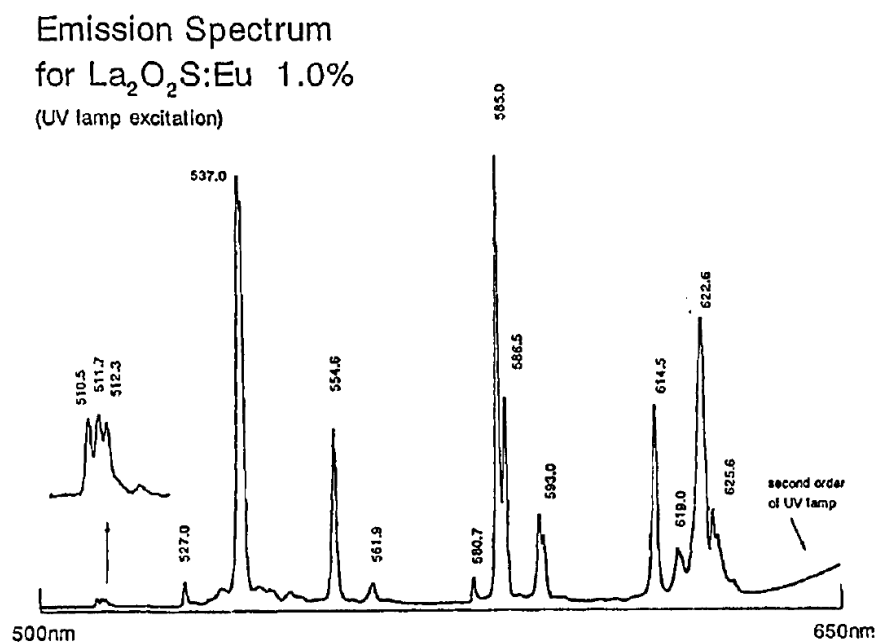


Figure 11: Emission intensity versus wavelength for $\text{La}_2\text{O}_2\text{S}:\text{Eu}$ phosphor at room temperature following 366 nm broadband excitation [4].

In figure 11 are shown the characteristic emission wavelengths for $\text{La}_2\text{O}_2\text{S}:\text{Eu}$ phosphor. The intensity distribution in the spectrum for UV lamp excitation is slightly different from that in the spectrum created by laser excitation, but the characteristic transitions are identical. Since, there is no calibrated y -axis, the intensity could be scaled logarithmic. Also, the spectral sensitivity may be different in our setup. The peaks and corresponding wavelengths of figure 11 were matched to the peaks of the CCD camera spectrum.

Figure 12 shall give an impression, how a raw spectrum looks like at the CCD chip.

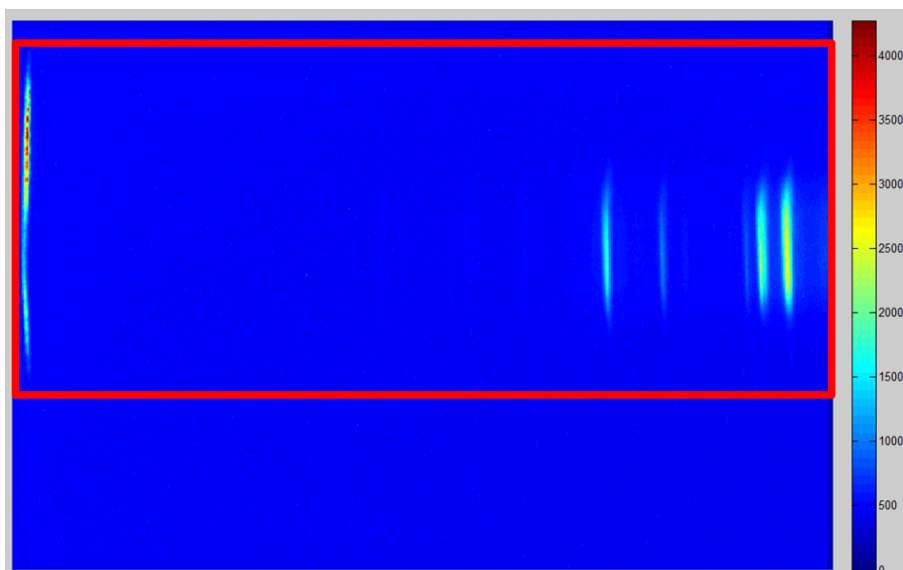


Figure 12: CCD raw image of a spectrum, that includes the laser peak (grating position is '690nm'), the red rectangle includes all CCD columns and shows the part of the image that is summed up column by column.

The color bar at the right hand side of figure 12 is an intensity scale for the pixel matrix. At 4300 units it is far from being saturated (absolute maximum value for intensity is 16383). That is why no non-linear saturation effects are expected.

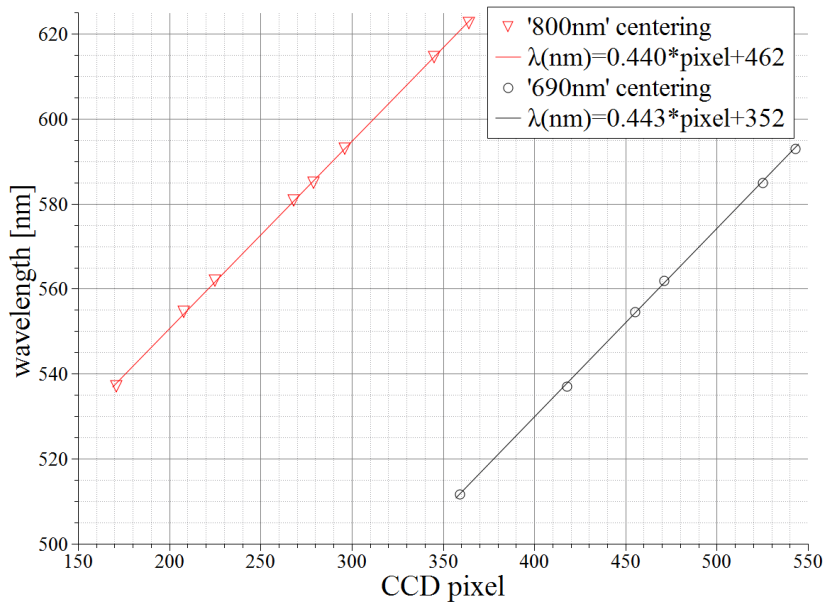


Figure 13: Wavelength calibration for the spectrometer's CCD camera image at the grating positions '800 nm' and '690 nm', matched by using literature values of figure 11. The grating positions or centerings do not follow a calibration, but are displayed at the grating controller (see table below).

Grating Controller Value	'800 nm'	'690 nm'
Spectrometer Range [nm]	253	255
Start and End Wavelength [nm]	462 ... 715	352 ... 607
Center of Range [nm]	589	480

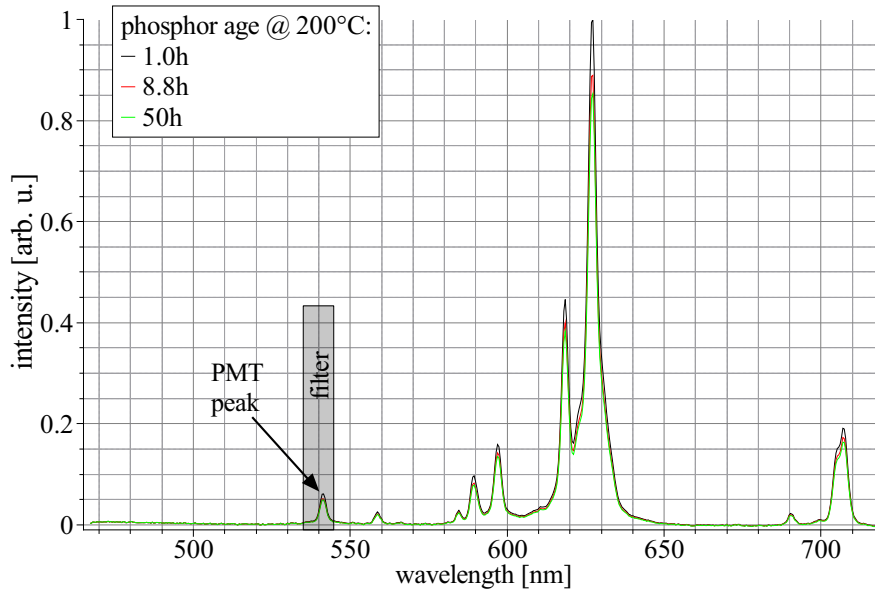


Figure 14: Phosphorescence spectra emitted by $\text{La}_2\text{O}_2\text{S}:\text{Eu}$ phosphor (8mass% Eu) after excitation at 355 nm. The time window has a length of $500\ \mu\text{s}$ and includes the laser peak (see 'blue window' in figure 16). Phosphor age as parameter, CCD gain = 4.5, Q-switch output delay = $-500\ \text{ns}$.

The spectra in figure 14 were recorded in parallel to the intensity decay curves in figure 6. The grey rectangle illustrates position and $FWHM = 10\ \text{nm}$ of the bandpass filter, that is used in front of the PMT. The grey part passes the filter, the other wavelengths are blocked. The spectra were recorded at a furnace temperature 200°C using the old sample holder. According to figure 9 it takes about 30 min to warm up the phosphor under this conditions. As a conclusion the phosphorescence spectra were chosen to have an age of more than 30 min.

The amplitudes of fitted exponential curves were taken to represent the decay intensities in figure 15. The spectral intensities were taken as the summed CCD column of the camera chip, that matches 540 nm.

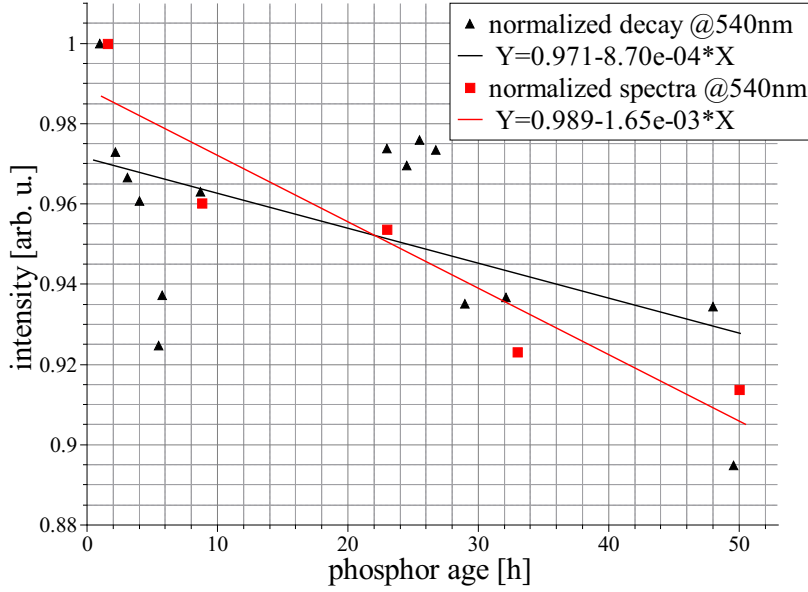


Figure 15: Comparison of the phosphorescence intensities at 540 nm, recorded by time decay investigation using the PMT (black) and time-gated spectral investigations using the CCD camera behind the spectrometer (red), Laser energy constant at 3 mJ.

In figure 15 the datasets show different slopes. The spectra intensity decreases almost twice as fast as the PMT intensity. The decay data points are more scattered. The RMSE (Root Mean Squared Error) equals 0.02335 for fitting to the decay. For fitting to the spectra datasets the RMSE equals 0.01391. That means, the confidence level of fitting a linear function to the spectra dataset is almost twice as high as for the decay dataset.

In spite of their uncertainty, the intensity values of PMT data follow a decreasing trend. Because the laser energy was kept constant all the time at 3 mJ, this trend is most likely caused by annealing of the $\text{La}_2\text{O}_2\text{S}:\text{Eu}$ (8mass%Eu) phosphor.

4.2.2 Trigger Delay for the CCD Camera

It is necessary to record CCD images including the time of the laser pulse on the one hand and without the laser pulse on the other hand to gain information about the spectral composition of the peak. The peak information one can get by subtracting the image without laser pulse from the image containing the laser pulse.

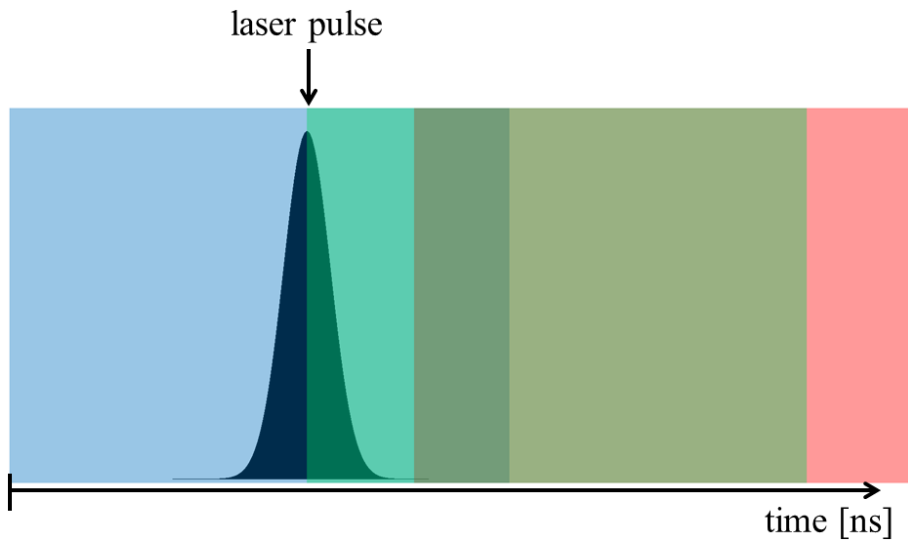


Figure 16: Schematic sketch of three types of time windows for the time-gated CCD camera: 'blue' includes the whole laser peak; 'green' cuts half of it and 'red' does not see any laser intensity at all.

In figure 16 are shown three different types of time windows for the CCD camera in principal. The blue time window starts several nanoseconds before the laser output. The green time window starts at the maximum laser intensity. The red time window starts a few nanoseconds after the laser peak. It is not possible to take an image just of the laser pulse, because the minimum exposure time of this CCD camera is limited to several microseconds. The time windows have to be of the same length, because of the noise level. The noise decreases, when the window is shortened.

The previous examples shall illustrate what was measured in figure 17.

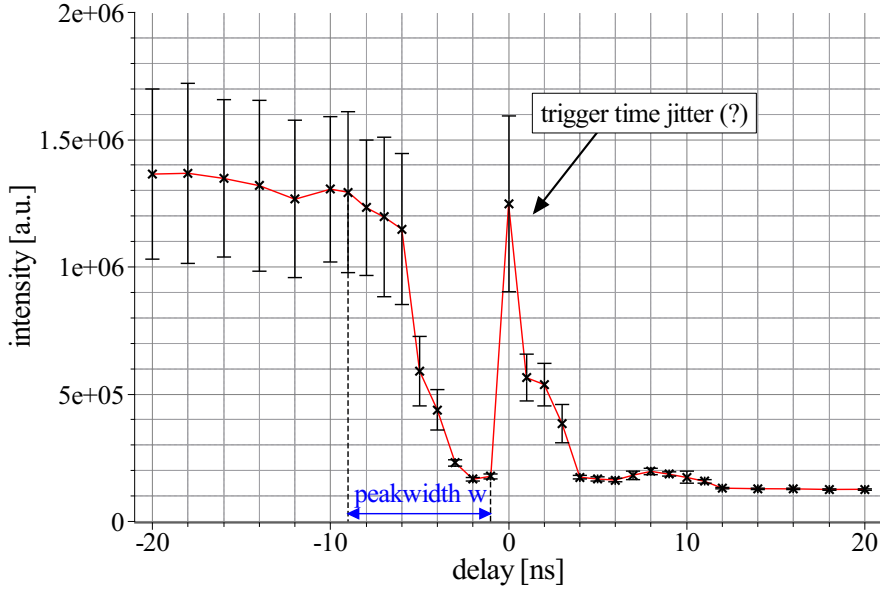


Figure 17: CCD intensity vs. Q-switch output delay. CCD columns were evaluated, that match the 355 nm laser emission line according to the wavelength calibration in 13

The delay on the x -axis in figure 17 is the position of the time window. For delays in the range of $[-20 \text{ ns}, -9 \text{ ns}]$ the blue window applies. The best representation for the green window is given by the point at delay -5 ns . Every time window is much longer than in the sketch of figure 16: they are $500 \mu\text{s}$ long. The intensity values are the integral over the laser peak. As the intensity decreases, the laser peak is cut more and more. When reaching the minimum, it is integrated over noise only and the time window is at the red position in figure 16.

The measurement of figure 17 is necessary in order to know for sure, at which time the laser peak will be recorded by the CCD camera and at which time the spectrum is not influenced by the laser peak, due to it is not recorded. The delay value for cutting the laser peak should be as short as possible, because the phosphorescence signal starts immediately after the laser pulse or even in parallel. Too long delays downgrade the phosphorescence signal to noise ratio.

In figure 17 the integrated signal (intensity [arb. u.]) increases from noise level back to the 'blue window' position. An explanation for this phenomenon is most likely the jitter error of the camera time window. That means that it is not possible to determine the delay of time window at an accuracy better than $\approx 10 \text{ ns}$, because the window may jump.

It follows from figure 17, that one is on the safe side, when choosing a Q-switch output delay of -10 ns to include the laser pulse and when choosing a Q-switch output delay of 6 ns to cut the laser pulse.

4.3 Time Decay Investigations at 538 nm Phosphor Emission

4.3.1 Influence of the Phosphor Preparation Time on the Intensity

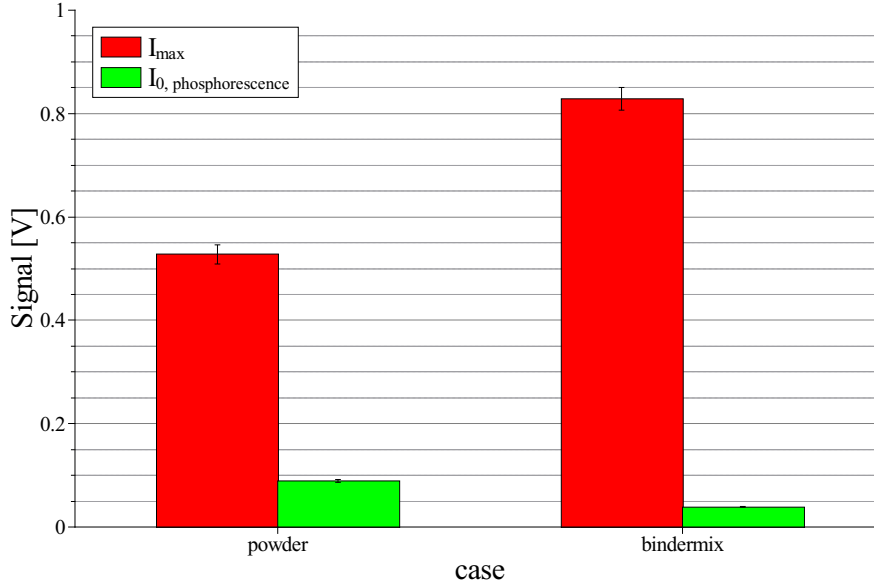


Figure 18: Comparison of two possibilities to coat $\text{La}_2\text{O}_2\text{S:Eu}$ phosphor, 2mass% Eu. In case of 'powder' the microcrystalline phosphor powder is mixed with methanol and HPC binder shortly before coating, the 'bindermix' is premixed once (phosphor powder and HPC binder) and used for several months.

In figure 18 the preparation of the phosphor has considerable influence on the recorded PMT signal. Although the laser peak (I_{max}) is stronger at the binder mix, the non-premixed powder delivers better results.

$$\frac{I_{max,powder}}{I_{max,bindermix}} = 0.64 \qquad \frac{I_{0,powder}}{I_{0,bindermix}} = 2.3$$

The powder has a I_0/I_{max} -ratio of 0.17. The binder mix has a I_0/I_{max} -ratio of 4.7×10^{-2} . The case 'powder' should be preferred.

However, there is no guarantee, that the layer thickness is the same in both cases, but it is very important when comparing two methods like this. If the phosphor layer is too thin, there will be less phosphorescence signal and more laser peak intensity. Probably the case 'bindermix' has too thin a layer of phosphor, because the mixture had have only a little amount left for coating.

4.3.2 Investigation of the Intensity Ratio between Peak and Phosphorescence from the PMT Decay Curves

The following graph in figure 19 summarizes the data of two series of measurements, evaluated by a MATLAB routine in terms of ratio.

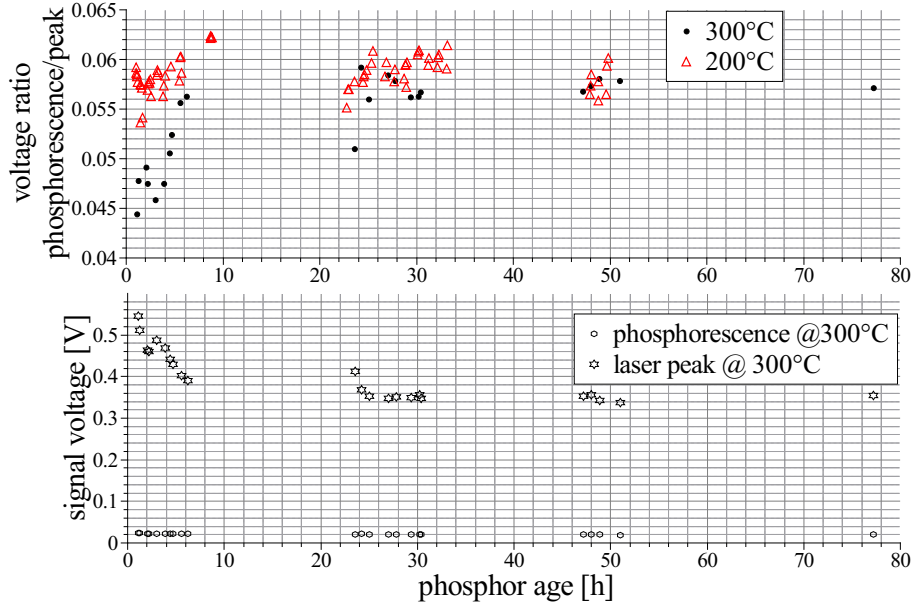


Figure 19: up: Ratios phosphorescence voltage / peak voltage, evaluated from data of two series of measurements at 300 °C (circles) and 200 °C (triangles) for constant laser energy = 3 mJ, PMT gain = 5.3 and europium concentration = 8mass% down: Signal values, evaluated for 300 °C as a function of phosphor age.

Figure 19 shows a trend of increase for the ratios, measured at 300 °C (black dots in this figure), while the data from 200 °C measurement hardly follow a considerable trend. In figure 19, down, it is obvious, that the changes in ratio are mainly caused by changes in the laser peak intensity. The calculated phosphorescence voltage (equivalent to I_0 in figure 15) is more stable than the maximum voltage (equivalent to I_{max} in figure 15), although the laser energy was kept constant at 3 mJ.

The considerable changes in ratio at 300 °C at the beginning are maybe caused by an annealing process, that does not take place at 200 °C.

The gaps in data along the time axis are due to the brakes or absence of work.

5 Summary and Outlook

In this work the experimental setup for measuring phosphor annealing processes was built up and step by step improved. Know-how was gained on how to operate the devices in the setup and processing the experimental data. After aligning and improving the setup some first phosphor tests were performed to prove the setups applicability.

Because the most considerable changes in the decay curves of the PMT occurred during the first hour after coating the phosphor (see figure 6), it was most relevant to measure the warm up time. The first sample holder prototype took about 30 minutes to adapt to 200 °C. The warm up process interferes the measurement signal. The warm up time should be decreased as far as possible to be able to start measurements earlier. It was replaced by an improved version, that drastically reduced the mass to heat up. This newer sample holder reduced the warm up time to 13 minutes, i.e. less than 50% compared to the original one. Measurements of several warm up times showed, that the time saving (improved holder + preheating) was even more efficient for adapting to 75 °C: less than 30% of the original warm up time.

It is described, how to process a CCD camera image to a wavelength calibrated spectrum. The comparison of spectrometer signals with the extrapolated phosphor intensity at $t = 0$ (mentioned as I_0) at 540 nm, recorded during the same series of measurement indicates a decrease for both, but the PMT data has half of the slope at higher statistical uncertainty (linear fitting).

The spectrometer's CCD camera has a jitter error of 10 ns. By intensity versus delay measurements it was also determined the Q-switch output delay: -10 ns to include and $+6$ ns to exclude the laser pulse in the CCD camera's time window.

The differences in maximum PMT intensities (I_{max}) and extrapolated phosphor intensities at $t = 0$ (I_0) between a premixed phosphor ('bindermix') and a phosphor, that is mixed shortly before coating ('powder') are probably caused by different layer thicknesses. While ratios (I_0/I_{max}) of phosphorescence and peak do not change by time considerably at 200 °C, there is a strong increase of ratio (I_0/I_{max}) at 300 °C within the first seven hours. Responsible for this phenomenon could be an annealing process.

The experimental setup is now ready for further investigations of the $\text{La}_2\text{O}_2\text{S}:\text{Eu}$ phosphor. The final goal of this research is to provide an application method for $\text{La}_2\text{O}_2\text{S}:\text{Eu}$ in thermometry.

The next steps will be measurements at higher temperatures for the 8mass% Eu phosphor, because it is promising to cover a lifetime range of 2-3 orders of magnitude.

For further reduction of the warming up time there should be built more and improved sample holders. It is also possible to think of a technique or method that is not dependent on the

furnace and not dependent on the holder, when the phosphor is coated directly on a thermal resistor.

It is desirable to automatize the setup by merging and controlling the process at the spectrometer and at the process at the oscilloscope in one PC and one software (e.g. Labview), because this would increase the efficiency in time of measurements and data evaluation dramatically.

The phenomenon of annealing at 300°C should be further investigated. A series of measurements at 350°C should show, if the annealing changes its speed. Also, it is desirable to record 100 decay curves per time and per temperature by the PMT in order to achieve higher accuracy for the data. This could help to understand or evaluate the phenomenon better, because the confidence level is raised and fitting functions will provide more reliable results.

References

- [1] M. R. Cates, S. W. Allison, L. Jaiswal, and D. L. Beshears. Yag:dy and yag:tm fluorescence to 1700 c. In *ISA - 49th International Instrumentation Symposium, 4-8 May, 2003*.
- [2] J.P. Feist, A.L. Heyes, and S. Seefeldt. Oxygen quenching of phosphorescence from thermographic phosphors. *Measurement Science and Technology*, 14:N17–N20, 2003.
- [3] A. H. Khalid and K. Kontis. Thermographic phosphors for high temperature measurements: Principles, current state of the art and recent applications. *Sensors*, 8:5673–5744, 2008.
- [4] R. H. Krauss, R. G. Hellier, and J. C. McDaniel. Surface temperature imaging below 300 k using $\text{La}_2\text{O}_2\text{S:eu}$. *APPLIED OPTICS*, 33:3901–3904, 1994.
- [5] G. Särner. *Laser-Induced Emission Techniques for Concentration and Temperature Probing in Combustion*. PhD thesis, Division of Combustion Physics, Department of Physics, Lund University, 2008.

Declaration of Authorship

I certify, that the work presented here is, to the best of my knowledge and belief, original and the results of my own investigations, except as referenced, and has not been submitted, either in part or whole, for this or any other Universities.

Lund, June 22nd 2011

Robert Koch